Contrasting Responses of Surface Heat Fluxes to Tropical Deforestation

Hung-Chen Chen[1] and Min-Hui Lo[2]

[1]Department of Atmospheric Sciences, National Taiwan University
[2]National Taiwan University

December 7, 2022

Abstract

Deforestation alters the exchange of heat, moisture, and momentum between the Earth's surface and the atmosphere, which can significantly affect the surface energy balance and water budget. However, changes in surface heat fluxes in response to deforestation are diverse among multi-model simulations. Changes in surface heat fluxes may lead to further energy partitioning and different land-atmosphere interactions. This study explores factors that might cause different changes in surface fluxes under tropical deforestation. The mediating effect of the Bowen ratio on changes in turbulent surface fluxes in response to the removal of tropical rainforests is examined with the Community Earth System Model of the National Center for Atmospheric Research. Different flux partitioning in the mean state of the Bowen ratio is associated with various flux changes under deforestation. When the mean Bowen ratio is smaller, deforestation tends to increase sensible heat fluxes and reduce latent heat fluxes. Our research further indicates that the simulated mean-state Bowen ratios in the Land Use Model Intercomparison Project model archive might modulate changes in surface heat fluxes that provide some clues for the land surface model developments.

Hosted file

`essoar.10512785.1.docx` available at https://authorea.com/users/563842/articles/610944-contrasting-responses-of-surface-heat-fluxes-to-tropical-deforestation

Contrasting Responses of Surface Heat Fluxes to Tropical Deforestation

Hung-Chen Chen[1] and Min-Hui Lo[1,2*]

[1]Department of Atmospheric Sciences, National Taiwan University, Taipei, Taiwan

[2]The International Degree Program in Climate Change and Sustainable Development, National Taiwan University, Taipei, Taiwan

*Corresponding author: Min-Hui Lo (minhuilo@ntu.edu.tw),

MIN-HUI LO (0000-0002-8653-143X) - ORCID

Key Points:

- Changes in surface heat fluxes in response to deforestation are diverse among climate models
- Deforestation under climate conditions with smaller Bowen ratios decreases latent heat fluxes and increases sensible heat fluxes
- The relationship between mean-state climate conditions and deforestation responses helps explain inconsistent results among climate models

Abstract

Deforestation alters the exchange of heat, moisture, and momentum between the Earth's surface and the atmosphere, which can significantly affect the surface energy balance and water budget. However, changes in surface heat fluxes in response to deforestation are diverse among multi-model simulations. Changes in surface heat fluxes may lead to further energy partitioning and different land-atmosphere interactions. This study explores factors that might cause different changes in surface fluxes under tropical deforestation. The mediating effect of the Bowen ratio on changes in turbulent surface fluxes in response to the removal of tropical rainforests is examined with the Community Earth System Model of the National Center for Atmospheric Research. Different flux partitioning in the mean state of the Bowen ratio is associated with various flux changes under deforestation. When the mean Bowen ratio is smaller, deforestation tends to increase sensible heat fluxes and reduce latent heat fluxes. Our research further indicates that the simulated mean-state Bowen ratios in the Land Use Model Intercomparison Project model archive might modulate changes in surface heat fluxes that provide some clues for the land surface model developments.

Plain Language Summary

Although deforestation in the tropics over the past few decades has been a driver of climate change, its effects on the climate are inconsistent among climate models. Through a series of sensitivity tests with land surface models, we found that mean-state climate conditions may modulate the effect of deforestation on the climate. Deforestation under climate conditions with smaller Bowen

ratios decreases latent heat fluxes and increases sensible heat fluxes. Mean-state climate conditions vary among multi-climate models, resulting in different responses to deforestation. The relationship between mean-state climate conditions and deforestation responses helps explain the inconsistent results among climate models.

1 Introduction

Tropical forests have experienced rapid deforestation over the past few decades (Rosa et al., 2016). Being one of the anthropogenic drivers of climate change, deforestation has three major effects on surface properties: (1) an increase in surface albedo, (2) a decrease in evapotranspiration efficiency, and (3) a decrease in surface roughness (Davin & de Noblet-Ducoudré, 2010). These changes in surface properties alter the exchange of momentum, heat, and moisture between the surface and the atmosphere. Through latent and sensible heat fluxes, the surface transfers absorb energy and moisture back to the atmosphere. This interaction between the surface and the atmosphere is important in determining the surface energy budget, hydrological cycle, boundary layer development, and local hydroclimate (Denissen et al., 2021; Santanello et al., 2018). Previous studies have shown that changes in evapotranspiration efficiency and surface roughness are two dominant processes in tropical forests (Davin & de Noblet-Ducoudré, 2010). Thus, the removal of tropical forests leads to an overall increase in surface temperature and the repartitioning of latent and sensible heat fluxes (Bell et al., 2015; L. Chen & Dirmeyer, 2020; Davin & de Noblet-Ducoudré, 2010; Laguë et al., 2019; Winckler et al., 2019).

Previous modeling studies have shown that although tropical deforestation consistently causes higher temperatures, it does not influence surface heat fluxes in a consistent manner (C.-C. Chen et al., 2019; Mabuchi et al., 2005a, 2005b; Schneck & Mosbrugger, 2011; Takahashi et al., 2017). Some idealized experiments such as those in the Land Use Model Intercomparison Project (LUMIP; Lawrence et al., 2016) have also yielded results (Fig. 1) regarding changes in surface heat fluxes that disagree with models in phase 6 of the Coupled Model Intercomparison Project (CMIP6; Eyring et al., 2016) (Boysen et al., 2020). This inconsistency in changes in surface heat fluxes highlights the difficulties in quantifying the effects of land use change on the climate and suggests that the underlying mechanisms of land-atmosphere interactions remain unclear. This study investigates the reasons for the inconsistency in changes in simulated surface fluxes to better quantify the effects of tropical deforestation on the local climate by conducting a series of NCAR Community Land Model experiments and analyzing results from LUMIP experiments.

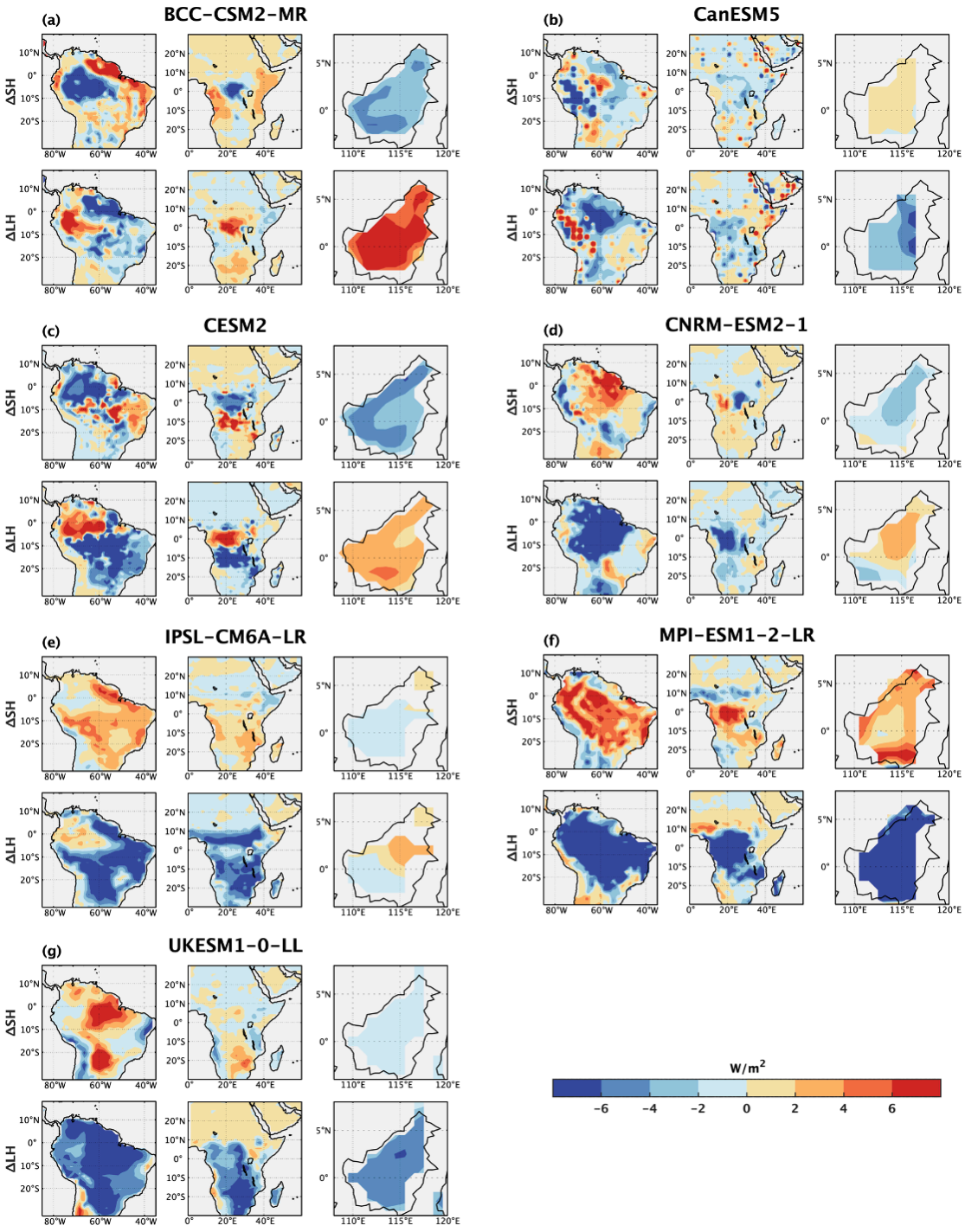
(a)
BCC-CSM2-MR
(b)
CanESM5
(c)
CESM2
(d)
CNRM-ESM2-1
(e)
IPSL-CM6A-LR
(f)
MPI-ESM1-2-LR
(g)
UKESM1-0-LL
ΔSH
ΔLH
W/m²
−6
−4
−2
0
2
4
6

Figure 1. Differences in sensible heat flux (SH) and latent heat flux (LH) between the LUMIP *deforest-glob* experiments (averaged over year 50 to year 80) and CMIP6 piControl experiments over South America, Africa, and Borneo.

2 Data and Methods

2.1 Experimental design

This study performed simulations using the Community Land Model version 4.0 (CLM4.0) in the Community Earth System Model version 1.0.3 with a horizontal resolution of 0.9° × 1.25°. To avoid excessive soil evaporation in CLM4.0 over the deforestation area, the soil evaporation resistance parameterization in CLM4.0 was replaced with dry surface layer-based soil resistances, as introduced in Swenson & Lawrence (2014). The offline simulations were forced with Global Soil Wetness Project Phase 3 (GSWP3; Hyungjun Kim, 2017). The air humidity in GSWP3 was modified to generate atmospheric forcings with the mean-state Bowen ratios of 0.24, 0.36, 0.41, and 0.45 over tropical forests. The four modified forcings were then used to perform sensitivity simulations representing the different climate states. Each modified forcing was used to drive two experiments: a control run and a deforestation run. In the deforestation runs, all the trees were replaced with C4 grasses. The difference between each of the four pairs of runs was calculated to show the effects of deforestation under different climate conditions.

2.2 Data

Deforest-glob is an idealized deforestation experiment within LUMIP in which 20 million km^2 of forest area is converted to grassland at a rate of 400,000 km^2/yr over a period of 50 years, followed by a period of at least 30 years with no changes in forest cover (Lawrence et al., 2016). Seven CMIP6 models participating in LUMIP were selected: BCC-CSM2-MR (Wu et al., 2019), CanESM5 (Swart et al., 2019), CESM2 (Danabasoglu et al., 2020), CNRM-ESM2-1 (Séférian et al., 2019), IPSL-CM6A-LR (Boucher et al., 2020), MPI-ESM1.2 (Mauritsen et al., 2019), and UKESM1-0-LL (Sellar et al., 2020). These models were selected because in these models, (1) leaf area indices decrease within the deforestation time period, and (2) variables required in this study are provided. The deforest-glob experiments carried out by these models and their corresponding piControl simulations were used for analysis. The piControl simulations and the final 30-year period (year 51 to year 80) of deforest-glob of the LUMIP archive were compared to analyze changes in surface heat fluxes. To better quantify the effects of deforestation, only grid cells for whom the loss of forest cover was greater than the median in each tropical forest were considered for analysis.

2.3 Analytical approach

The changes over three tropical forests (i.e., Amazon, Congo, and Borneo) were analyzed in this study. River basin masks of Amazon and Congo from the Information on Total Runoff Integrating Pathways (TRIP; Oki & Sud, 1998) were used. Results from both offline sensitivity tests and LUMIP experiments were analyzed by mixing the data from each grid cell together to explore the relationship between climate conditions and change in fluxes. By mixing together the signal of each grid cell from seven LUMIP models, we could explore the reasons for the inconsistency in the flux changes among models.

Water-limited and energy-limited conditions for each grid cell were evaluated with the equation established in Denissen (2020):

$$\text{corr} = \text{corr}\left(ET^{'}, Ts^{'}\right) - \text{corr}\left(ET^{'}, Sm^{'}\right). \qquad ---(1)$$

The Bowen ratio (the ratio of sensible heat flux to latent heat flux)

$$\text{Bowen ration} = \frac{\text{SH}}{\text{LH}}. \qquad ---(2)$$

3 Results

3.1 Offline CLM sensitivity tests

The offline CLM sensitivity tests indicated a relationship between the Bowen ratio and changes in the surface heat fluxes (Fig. 2). The scatter plots are the differences in the surface heat fluxes between the deforestation and control runs of each grid cell in the CLM experiments (Fig. 2a–f). The Bowen ratio was directly and inversely proportional to changes in latent heat fluxes and sensible heat fluxes, respectively, but as the Bowen ratio became greater, its influence on changes in latent heat fluxes became less pronounced. Figures 2g–l also indicate differences in altered surface heat fluxes in response to different mean-state climate conditions. Grid cells with Bowen ratios below the first quartile tended to have greater sensible heat fluxes and smaller latent heat fluxes after deforestation, whereas grid cells with Bowen ratios above the third quartile tended to have smaller sensible heat fluxes and slightly smaller latent heat fluxes after deforestation. That is, deforestation tended to increase sensible heat fluxes and decrease latent heat fluxes when it occurred in a climate with a smaller Bowen ratio. By contrast, it tended to decrease the sensible heat fluxes and have a minor influence on the latent heat fluxes when it occurred in a climate with a greater Bowen ratio.

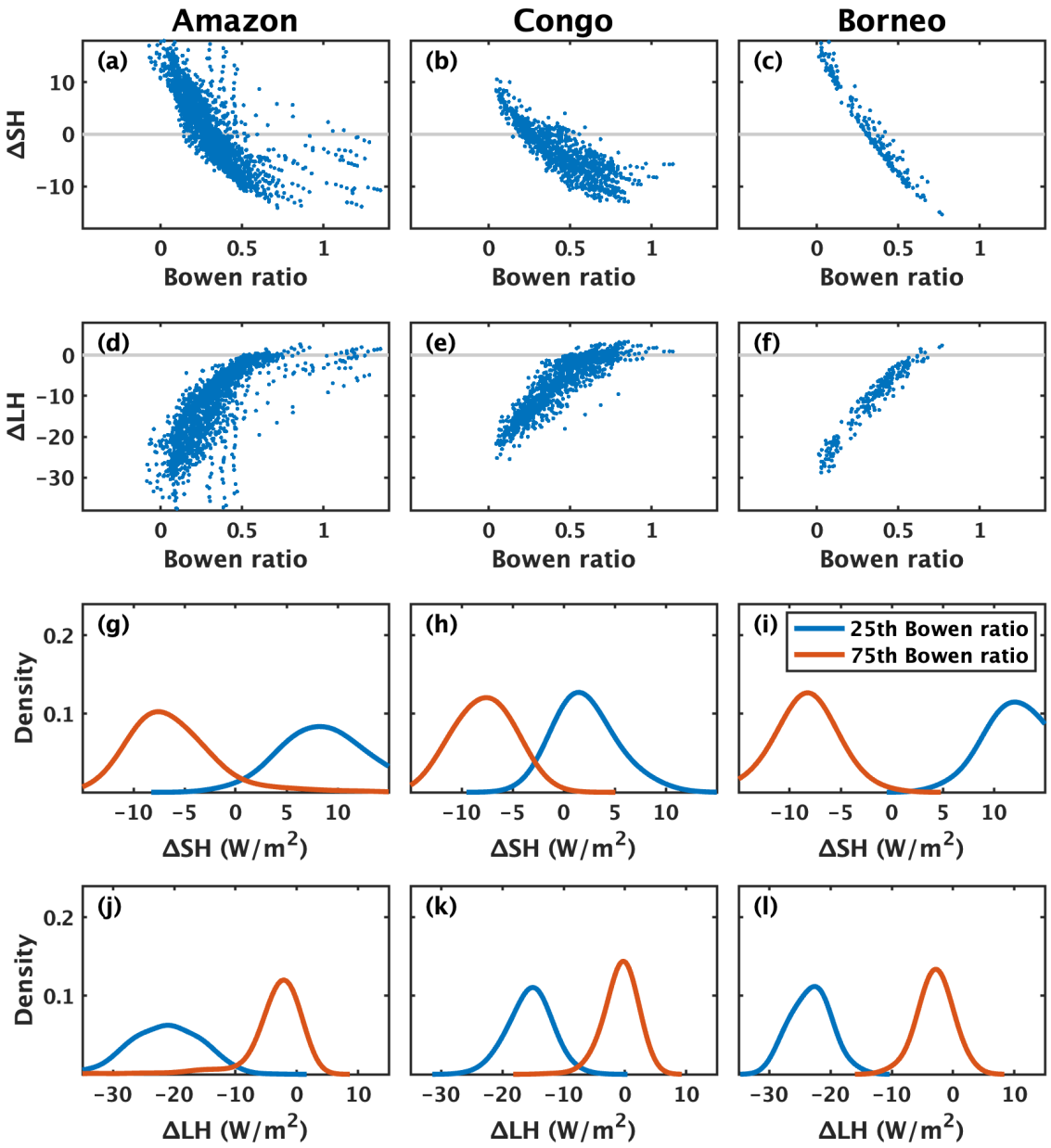

Figure 2. Relationship between Bowen ratio and changes in surface heat fluxes over tropical forests in offline simulations driven by atmospheric forcings with different Bowen ratios. (a-c) Relationship between Bowen ratio and change in sensible heat flux (SH). (d-f) Relationship between Bowen ratio and change in latent heat flux (LH).

(g-i) Probability density of change in sensible heat flux (SH). (j-l) Probability density of change in latent heat flux (LH). Blue lines show the changes when the mean-state Bowen ratio is below the first quartile in the control run, and red lines show the changes when the mean-state Bowen ratio is above the third quartile in the control run.

To explore the mechanism underlying the relationship between changes in the surface heat fluxes and mean-state conditions, we analyzed how the aforementioned two dominant processes, evapotranspiration efficiency and surface roughness, affect the surface heat fluxes in the tropics (Fig. 3). Sensible and latent heat fluxes are turbulent fluxes featuring the exchange of energy between the surface and the atmosphere through turbulent mixing. The efficiency of turbulent fluxes is proportional to the roughness length. Deforestation reduces roughness length and results in a smaller frictional velocity and greater aerodynamic resistance, leading to a repartitioning of surface heat fluxes and longwave radiation. A smaller roughness length under deforestation makes it difficult for the surface to exchange energy with the atmosphere through turbulent mixing. Therefore, the surface temperature increases to emit more longwave radiation to remove energy from the surface and maintain the surface energy balance. This is consistent with Bell et al., 2015; Boysen et al., 2020; Laguë et al., 2019; Nelli et al., 2020; Winckler et al., 2017, 2019.

Figure 3 also shows how deforestation alters surface heat fluxes by decreasing evapotranspiration efficiency. Transpiration resistance is controlled by vegetation types. Replacing forests with grassland reduces transpiration and results in higher soil water content. Deforestation reduces leaf area, resulting in smaller amounts of stomata, less intercepted water, and reduced canopy evapotranspiration. The smaller leaf area increases the amount of shortwave radiation absorbed by the soil, which can increase the amount of soil evaporation in more energy-limited regions such as tropical forests. In addition to allowing the soil to receive more energy, a smaller leaf area also increases the amount of throughfall and thus the amount of soil moisture. The higher soil water content due to reduced transpiration and reduced leaf area favors soil evaporation. Changes in transpiration, canopy evaporation, and soil evaporation can influence the latent heat fluxes. As the latent heat flux is altered, the sensible heat flux simultaneously adjusts to maintain the surface energy balance. Both roughness length and evapotranspiration efficiency affect surface heat fluxes, and deforestation may result in varying flux through the interaction between the two mechanisms.

The table shown at the bottom of Fig. 3 displays the responses of surface fluxes to deforestation in Borneo from sensitivity tests with the greatest and

the smallest Bowen ratios. In the simulation with the smallest Bowen ratio, the significant decrease in transpiration dominates the change in latent heat fluxes. This decrease in latent heat fluxes leads to an increase in sensible heat fluxes to maintain surface energy balance. In the simulation with the greatest Bowen ratio, the decrease in transpiration was not as significant and was compensated by an increase in soil evaporation; thus, sensible heat fluxes did not need to increase for the surface energy balance to be maintained. Consequently, deforestation leads to reductions in both surface heat fluxes when the Bowen ratio is greater. Similar results can be seen for Congo and the Amazon.

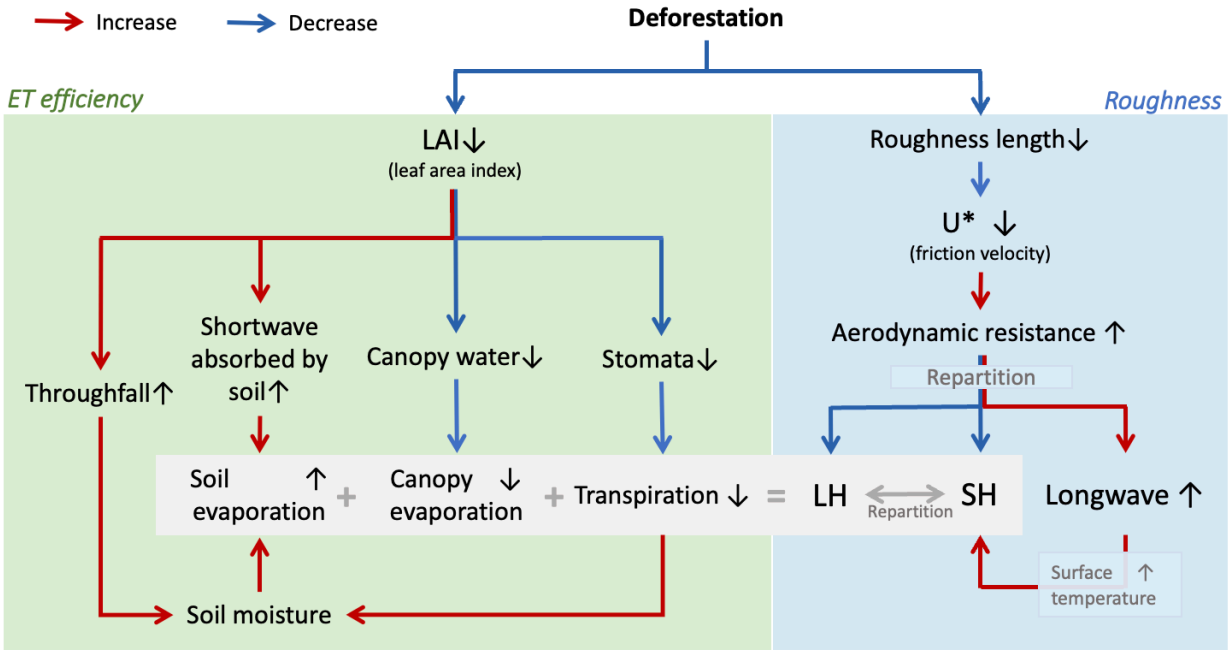

Experiment	Ground evaporation	Canopy evaporation	Transpiration	Latent heat flux	Sensible heat flux
Bowen ratio = 0.09	+11.42 ± 5.35	-5.17 ± 2.61	-29.57 ± 5.46	-23.32 ± 2.81	+12.26 ± 2.76
Bowen ratio = 0.51	+11.29 ± 4.62	-5.03 ± 2.56	-10.23 ± 4.54	-3.96 ± 3.07	-7.01 ± 3.43

w/m^2

Figure 3. How deforestation influences surface heat fluxes. The table shows average changes in fluxes between deforestation and control runs over Borneo in the experiments with the smallest and the greatest Bowen ratios. The green box illustrates the mechanism of evapotranspiration efficiency. The blue box illustrates the mechanism of surface roughness. The gray box illustrates the interaction between these two mechanisms.

3.2 LUMIP experiments

> Similar but weaker relationships between mean-state flux partitioning (i.e., Bowen ratio) and the flux changes in response to deforestation can also be observed in LUMIP experiments (Fig. 4). Deforestation is more likely to increase sensible heat fluxes and decrease latent heat fluxes at grid cells with lower Bowen ratios (Fig. 4a–f). By contrast, deforestation is more likely to decrease sensible heat fluxes and increase latent heat fluxes at grid cells with higher Bowen ratios. That is, models with smaller mean-state Bowen ratios are more likely to have an increase in sensible heat fluxes and a decrease in latent heat fluxes. The flux changes in different Bowen ratios for Congo and the Amazon were not as distinct as that for Borneo. This may suggest that the nonlocal adjustment to deforestation is stronger for Congo and the Amazon.

Regions with sufficient precipitation and less radiation are characterized as energy-limited, whereas regions with less precipitation and more radiation are characterized as water-limited (Denissen et al., 2020; Konapala et al., 2020; Ryu et al., 2008). Energy-limited regions are generally wetter and have higher soil water content. With sufficient available water, energy-limited regions tend to have greater latent heat fluxes and hence lower Bowen ratios. Conversely, water-limited regions are usually drier, tend to have smaller latent heat fluxes, and thus have higher Bowen ratios (Denissen et al., 2021). As shown in Fig. 4g–h, grid cells with higher Bowen ratios were more water-limited in Congo and the Amazon. However, in Borneo, the corr of grid cells with different Bowen ratios were comparable (Fig. 4i) and were higher than those in Congo and the Amazon. With the highest annual precipitation among the three tropical forests, Borneo is overall more energy-limited. In addition, the corr of grid cells with Bowen ratios above the third quartile in Borneo were significantly higher than those in Amazon ($P < .001$) and Congo ($P < .001$). This is due to the land-sea distribution pattern in Borneo, in which higher surface temperatures induce lateral water vapor transport to Borneo from the surrounding oceans (Fig. 4j). Therefore, grid cells with Bowen ratios above the third quartile in Borneo were also more energy-limited than those for Congo and the Amazon.

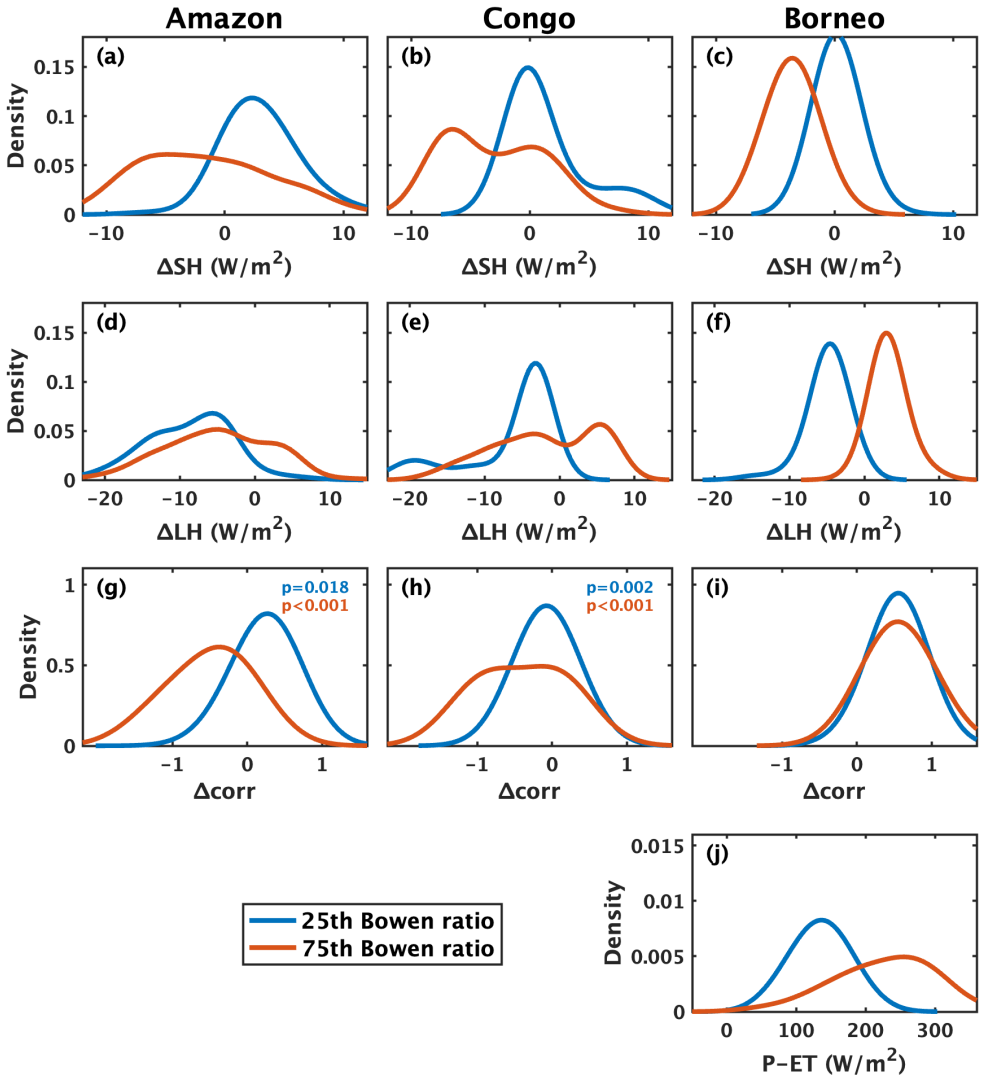

Figure 4. Changes in surface heat fluxes and water and energy conditions in the LUMIP model simulations. (a-f) Similar to Figure 4, but for the LUMIP deforest-glob and CMIP6 piControl experiments. The probability density of (g-i) corr over tropical forests and (j) the moisture convergence over Borneo in CMIP6 piControl experiments. Blue lines show changes with the mean-state Bowen ratio below the first quartile in the control run, and red lines show the responses with the mean-state Bowen ratio above the third quartile in the control run. The statistical significance of the difference between corr of Amazon and Borneo and between corr of Congo and Borneo are

shown in (g) and (h).

4 Discussion and Conclusions

The sensitivity tests showed that the mean-state partitioning of surface heat fluxes affects change in surface heat fluxes in response to deforestation. The near-surface vertical humidity gradient is related to the decrease in the amount of transpiration. A greater reduction in transpiration is the dominant mechanism underlying changes in latent heat flux, therefore leading to an increase in sensible heat flux to compensate for the change in the surface energy balance. A slighter decrease in transpiration and the compensation from the increase in soil evaporation results in a smaller decrease in latent heat fluxes, leading to a decrease in sensible heat fluxes. The decrease in transpiration and increase in soil evaporation affect the change in latent heat fluxes, and the change in latent heat fluxes determines whether sensible heat fluxes will increase to maintain the energy balance. The model simulations indicated that the inconsistency in changes in fluxes in response to deforestation may be related to the mean-state conditions. The results of this study may be crucial to explaining the inconsistency in flux responses between climate models and advancing our understanding of the effects of deforestation on the local climate.

Despite having similar results as offline sensitivity tests, LUMIP simulations had less distinct changes in surface heat fluxes for different mean-state conditions. In fully coupled simulations, both atmospheric conditions and sea surface temperature adjust accordingly to changes in the land surface conditions. In addition, changes in surface heat fluxes for different mean-state conditions differed between tropical forests. Borneo had the most significant changes in surface heat fluxes. This may suggest that climate feedbacks through changes in ocean and atmospheric conditions are stronger over Congo and the Amazon. Hence, signals in LUMIP experiments are not as clear as those in offline simulations.

The relationship between the mean-state Bowen ratio and the change in flux for each CMIP6 model is shown in Fig. S1–S3. Although a relationship similar to the results from offline simulations can be seen when the signal of each grid cell from LUMIP experiments is mixed, not all models indicate a similar relationship. In general, models or grid cells with a mean-state Bowen ratio above the third quartile tended to show greater decreases in sensible heat fluxes and increases in latent heat fluxes. Models or grid cells with a mean-state Bowen ratio below the third quartile tended to show greater increases in sensible heat fluxes and decreases in latent heat fluxes. However, some models exhibited opposite tendencies or diverse changes in fluxes under similar mean-state flux partitioning, such as BCC, CanESM, and CESM2 over the Amazon, and IPSL and UK over Congo. The relationship between the Bowen ratio and the change in surface heat fluxes may explain why models differ with respect to changes in surface heat fluxes. The varying rates of precipitation, net radiation, surface resistance, land-atmosphere coupling strength, and initial forest cover may lead to various mean-state conditions across models and further lead to varying responses to deforestation.

Acknowledgments

This study was supported by the National Science and Technology Council grant 110-2628-M-002-004MY4 to National Taiwan University. The river basin mask is provided by Total Runoff Integrating Pathways on the website (http://hydro.iis.u-tokyo.ac.jp/~taikan/TRIPDATA/). We also thank Dr. Marysa Laguë for fruitful discussions and advice on the effect of roughness and turbulent fluxes.

Data and code availability

All results were analyzed by using Python 3.8.10 and visualized by using MATLAB R2021a. The data and the codes for analyses are compiled on the Zenodo data repository (https://doi.org/10.5281/zenodo.7106480).

References

Bell, J. P., Tompkins, A. M., Bouka-Biona, C., & Sanda, I. S. (2015). A process-based investigation into the impact of the Congo basin deforestation on surface climate. *Journal of Geophysical Research: Atmospheres*, *120*(12), 5721–5739. https://doi.org/https://doi.org/10.1002/2014JD022586

Boucher, O., Servonnat, J., Albright, A. L., Aumont, O., Balkanski, Y., Bastrikov, V., Bekki, S., Bonnet, R., Bony, S., Bopp, L., Braconnot, P., Brockmann, P., Cadule, P., Caubel, A., Cheruy, F., Codron, F., Cozic, A., Cugnet, D., D'Andrea, F., … Vuichard, N. (2020). Presentation and Evaluation of the IPSL-CM6A-LR Climate Model. *Journal of Advances in Modeling Earth Systems*, *12*(7). https://doi.org/10.1029/2019MS002010

Boysen, L. R., Brovkin, V., Pongratz, J., Lawrence, D. M., Lawrence, P., Vuichard, N., Peylin, P., Liddicoat, S., Hajima, T., Zhang, Y., Rocher, M., Delire, C., Séférian, R., Arora, V. K., Nieradzik, L., Anthoni, P., Thiery, W., Laguë, M. M., Lawrence, D., & Lo, M.-H. (2020). Global climate response to idealized deforestation in CMIP6 models. *Biogeosciences*, *17*(22), 5615–5638. https://doi.org/10.5194/bg-17-5615-2020

Chen, C.-C., Lo, M.-H., Im, E.-S., Yu, J.-Y., Liang, Y.-C., Chen, W.-T., Tang, I., Lan, C.-W., Wu, R.-J., & Chien, R.-Y. (2019). Thermodynamic and Dynamic Responses to Deforestation in the Maritime Continent: A Modeling Study. *Journal of Climate*, *32*(12), 3505–3527. https://doi.org/10.1175/JCLI-D-18-0310.1

Chen, L., & Dirmeyer, P. A. (2020). Reconciling the disagreement between observed and simulated temperature responses to deforestation. *Nature Communications*, *11*(1), 202. https://doi.org/10.1038/s41467-019-14017-0

Danabasoglu, G., Lamarque, J.-F., Bacmeister, J., Bailey, D. A., DuVivier, A. K., Edwards, J., Emmons, L., Fasullo, J., Garcia, R., Gettelman, A., Hannay, C., Holland, M. M., Large, W. G., Lauritzen, P., Lawrence, D. M., Lenaerts, J., Lindsay, K., Lipscomb, W., Mills, M. J., & Strand, W. G. (2020). The

Community Earth System Model version 2 (CESM2). *Journal of Advances in Modeling Earth Systems*, *12*. https://doi.org/10.1029/2019MS001916

Davin, E. L., & de Noblet-Ducoudré, N. (2010). Climatic Impact of Global-Scale Deforestation: Radiative versus Nonradiative Processes. *Journal of Climate*, *23*(1), 97–112. https://doi.org/10.1175/2009JCLI3102.1

Denissen, J. M. C., Orth, R., Wouters, H., Miralles, D. G., van Heerwaarden, C. C., de Arellano, J. V.-G., & Teuling, A. J. (2021). Soil moisture signature in global weather balloon soundings. *Npj Climate and Atmospheric Science*, *4*(1), 13. https://doi.org/10.1038/s41612-021-00167-w

Denissen, J. M. C., Teuling, A. J., Reichstein, M., & Orth, R. (2020). Critical Soil Moisture Derived From Satellite Observations Over Europe. *Journal of Geophysical Research: Atmospheres*, *125*(6). https://doi.org/10.1029/2019JD031672

Eyring, V., Bony, S., Meehl, G. A., Senior, C. A., Stevens, B., Stouffer, R. J., & Taylor, K. E. (2016). Overview of the Coupled Model Intercomparison Project Phase 6 (CMIP6) experimental design and organization. *Geoscientific Model Development*, *9*(5), 1937–1958. https://doi.org/10.5194/gmd-9-1937-2016

Hyungjun Kim. (2017). Global Soil Wetness Project Phase 3 Atmospheric Boundary Conditions (Experiment 1). *Data Integration and Analysis System (DIAS)*.

Konapala, G., Mishra, A. K., Wada, Y., & Mann, M. E. (2020). Climate change will affect global water availability through compounding changes in seasonal precipitation and evaporation. *Nature Communications*, *11*(1), 3044. https://doi.org/10.1038/s41467-020-16757-w

Laguë, M. M., Bonan, G. B., & Swann, A. L. S. (2019). Separating the Impact of Individual Land Surface Properties on the Terrestrial Surface Energy Budget in both the Coupled and Uncoupled Land–Atmosphere System. *Journal of Climate*, *32*(18), 5725–5744. https://doi.org/10.1175/JCLI-D-18-0812.1

Lawrence, D. M., Hurtt, G. C., Arneth, A., Brovkin, V., Calvin, K. v, Jones, A. D., Jones, C. D., Lawrence, P. J., de Noblet-Ducoudré, N., Pongratz, J., Seneviratne, S. I., & Shevliakova, E. (2016). The Land Use Model Intercomparison Project (LUMIP) contribution to CMIP6: rationale and experimental design. *Geoscientific Model Development*, *9*(9), 2973–2998. https://doi.org/10.5194/gmd-9-2973-2016

Mabuchi, K., Sato, Y., & Kida, H. (2005a). Climatic Impact of Vegetation Change in the Asian Tropical Region. Part I: Case of the Northern Hemisphere Summer. *Journal of Climate*, *18*(3), 410–428. https://doi.org/10.1175/JCLI-3273.1

Mabuchi, K., Sato, Y., & Kida, H. (2005b). Climatic Impact of Vegetation Change in the Asian Tropical Region. Part II: Case of the Northern Hemisphere Winter and Impact on the Extratropical Circulation. *Journal of Climate*, *18*(3), 429–446. https://doi.org/10.1175/JCLI-3274.1

Mauritsen, T., Bader, J., Becker, T., Behrens, J., Bittner, M., Brokopf, R., Brovkin, V., Claussen, M., Crueger, T., Esch, M., Fast, I., Fiedler, S., Fläschner, D., Gayler, V., Giorgetta, M., Goll, D. S., Haak, H., Hagemann, S., Hedemann, C., … Roeckner, E. (2019). Developments in the MPI-M Earth System Model version 1.2 (MPI-ESM1.2) and Its Response to Increasing CO2. *Journal of Advances in Modeling Earth Systems*, *11*(4), 998–1038. https://doi.org/10.1029/2018MS001400

Nelli, N. R., Temimi, M., Fonseca, R. M., Weston, M. J., Thota, M. S., Valappil, V. K., Branch, O., Wulfmeyer, V., Wehbe, Y., al Hosary, T., Shalaby, A., al Shamsi, N., & al Naqbi, H. (2020). Impact of Roughness Length on WRF Simulated Land-Atmosphere Interactions Over a Hyper-Arid Region. *Earth and Space Science*, *7*(6), e2020EA001165. https://doi.org/https://doi.org/10.1029/2020EA001165

Oki, T., & Sud, Y. C. (1998). Design of Total Runoff Integrating Pathways (TRIP)—A Global River Channel Network. *Earth Interactions*, *2*(1), 1–37. https://doi.org/10.1175/1087-3562(1998)002<0001:DOTRIP>2.3.CO;2

Rosa, I. M. D., Smith, M. J., Wearn, O. R., Purves, D., & Ewers, R. M. (2016). The Environmental Legacy of Modern Tropical Deforestation. *Current Biology*, *26*(16), 2161–2166. https://doi.org/https://doi.org/10.1016/j.cub.2016.06.013

Ryu, Y., Baldocchi, D. D., Ma, S., & Hehn, T. (2008). Interannual variability of evapotranspiration and energy exchange over an annual grassland in California. *Journal of Geophysical Research: Atmospheres*, *113*(D9). https://doi.org/https://doi.org/10.1029/2007JD009263

Santanello, J. A., Dirmeyer, P. A., Ferguson, C. R., Findell, K. L., Tawfik, A. B., Berg, A., Ek, M., Gentine, P., Guillod, B. P., van Heerwaarden, C., Roundy, J., & Wulfmeyer, V. (2018). Land–Atmosphere Interactions: The LoCo Perspective. *Bulletin of the American Meteorological Society*, *99*(6), 1253–1272. https://doi.org/10.1175/BAMS-D-17-0001.1

Schneck, R., & Mosbrugger, V. (2011). Simulated climate effects of Southeast Asian deforestation: Regional processes and teleconnection mechanisms. *J. Geophys. Res.*, *116*, D11116. https://doi.org/10.1029/2010JD015450

Séférian, R., Nabat, P., Michou, M., Saint-Martin, D., Voldoire, A., Colin, J., Decharme, B., Delire, C., Berthet, S., Chevallier, M., Sénési, S., Franchisteguy, L., Vial, J., Mallet, M., Joetzjer, E., Geoffroy, O., Guérémy, J. F., Moine, M. P., Msadek, R., … Madec, G. (2019). Evaluation of CNRM Earth System Model, CNRM-ESM2-1: Role of Earth System Processes in Present-Day and Future Climate. *Journal of Advances in Modeling Earth Systems*, *11*(12), 4182–4227. https://doi.org/10.1029/2019MS001791

Sellar, A. A., Walton, J., Jones, C. G., Wood, R., Abraham, N. L., Andrejczuk, M., Andrews, M. B., Andrews, T., Archibald, A. T., de Mora, L., Dyson, H., Elkington, M., Ellis, R., Florek, P., Good, P., Gohar, L., Haddad, S., Hardiman, S. C., Hogan, E., … Griffiths, P. T. (2020). Implementation of U.K. Earth

System Models for CMIP6. *Journal of Advances in Modeling Earth Systems*, *12*(4). https://doi.org/10.1029/2019MS001946

Swart, N. C., Cole, J. N. S., Kharin, V. v, Lazare, M., Scinocca, J. F., Gillett, N. P., Anstey, J., Arora, V., Christian, J. R., Hanna, S., Jiao, Y., Lee, W. G., Majaess, F., Saenko, O. A., Seiler, C., Seinen, C., Shao, A., Sigmond, M., Solheim, L., … Winter, B. (2019). The Canadian Earth System Model version 5 (CanESM5.0.3). *Geoscientific Model Development*, *12*(11), 4823–4873. https://doi.org/10.5194/gmd-12-4823-2019

Swenson, S. C., & Lawrence, D. M. (2014). Assessing a dry surface layer-based soil resistance parameterization for the Community Land Model using GRACE and FLUXNET-MTE data. *Journal of Geophysical Research: Atmospheres*, *119*(17), 10, 210–299, 312. https://doi.org/https://doi.org/10.1002/2014JD022314

Takahashi, A., Kumagai, T., Kanamori, H., Fujinami, H., Hiyama, T., & Hara, M. (2017). Impact of tropical deforestation and forest degradation on precipitation over Borneo island. *J. Hydrometeor.*, *18*, 2907–2922. https://doi.org/10.1175/JHM-D-17-0008.1

Winckler, J., Reick, C. H., Bright, R. M., & Pongratz, J. (2019). Importance of Surface Roughness for the Local Biogeophysical Effects of Deforestation. *Journal of Geophysical Research: Atmospheres*, *124*(15), 8605–8618. https://doi.org/10.1029/2018JD030127

Winckler, J., Reick, C. H., & Pongratz, J. (2017). Robust Identification of Local Biogeophysical Effects of Land-Cover Change in a Global Climate Model. *Journal of Climate*, *30*(3), 1159–1176. https://doi.org/10.1175/JCLI-D-16-0067.1

Wu, T., Lu, Y., Fang, Y., Xin, X., Li, L., Li, W., Jie, W., Zhang, J., Liu, Y., Zhang, L., Zhang, F., Zhang, Y., Wu, F., Li, J., Chu, M., Wang, Z., Shi, X., Liu, X., Wei, M., … Liu, X. (2019). The Beijing Climate Center Climate System Model (BCC-CSM): the main progress from CMIP5 to CMIP6. *Geoscientific Model Development*, *12*(4), 1573–1600. https://doi.org/10.5194/gmd-12-1573-2019